

Synthesis of Triazine Derivative and Its Application in the Modification of Cellulose Nanocrystals

Yuanyuan Yin,^{a,b} Lina Zhao,^b Xue Jiang,^{a,b,*} Hongbo Wang,^{a,b,*} and Weidong Gao^{a,b}

Cellulose nanocrystals (CNCs) were modified with triazine derivative in an effort to decrease the hydrophilicity of CNCs and improve their thermal stability. In recent decades, much attention has been given to the modification of CNCs to broaden their use in various applications, such as in nanocomposites, as adsorbents for the disposal of wastewater, and so on. The CNCs with a rod-like shape were obtained from cotton through sulfuric acid hydrolysis. Hydrophobic triazine derivative was synthesized *via* the reaction between triazine and *n*-butylamine (BA) and then applied to modify CNCs to improve their thermal stability and diminish the hydrophilicity of the nanoparticles. Results of thermogravimetric analysis (TGA) indicated a 150 °C increase in the initial thermal decomposition temperature of modified nanocrystals compared to the original CNCs. The improved thermal stability of modified CNCs was attributed to a shielding effect of the hydrophobic aliphatic amine layer on the surface of the nanoparticles. The results of the dynamic contact angle measurement revealed a decrease of hydrophilicity of the modified CNCs.

Keywords: Cellulose nanocrystals; Triazine derivative; Thermal stability; Hydrophilicity

Contact information: a: Jiangsu Engineering and Technology Research Center for Functional Textiles, Jiangnan University, Wuxi, Jiangsu 214122, China; b: Key Laboratory of Eco-textiles of Ministry of Education, Jiangnan University, Wuxi, Jiangsu 214122, China;

* Corresponding authors: jiangx@jiangnan.edu.cn; wxwanghb@163.com

INTRODUCTION

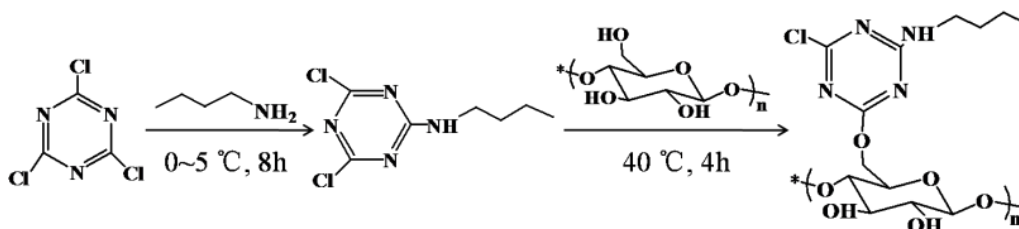
Cellulose, as one of the most abundant renewable polymer resources in the world, has aroused much attention as an engineering material (Zhang *et al.* 2015). Emerging uses of cellulose include the adsorption of pollutants from aqueous solutions (Annadurai *et al.* 2002) and in the medical field (Klemm *et al.* 2001). Formed by the repeated connection of β -D-glucose building blocks linked by β -1,4-glycosidic bonds, cellulose can be thoroughly degraded into water and carbon dioxide (Jokerst *et al.* 2014; Liu *et al.* 2014). Nanocellulose can be obtained from cellulose using acid hydrolysis (Bake *et al.* 2013; Chen *et al.* 2015; Guo *et al.* 2016), enzymolysis, and mechanical pulverizing. The main process for the isolation of CNCs from cellulose is based on acid hydrolysis. The CNCs are obtained because the amorphous regions of cellulose are susceptible to hydrolysis and may be degraded and dissolved, leaving the rigid crystalline regions.

In the past, CNCs, as an ideal reinforcer, have attracted notice in the field of nanocomposites, attributable to their biodegradability, light weight, nanocrystal size, low cost, high specific strength and modulus (100 GPa in the axial crystalline regions) (Iwamoto *et al.* 2009; Berglun 2010), unique morphology, and relatively reactive surface (Habibi *et al.* 2008; Azouz *et al.* 2012; Lin and Dufresne 2013; Liu *et al.* 2015). Nevertheless, there are two challenges to overcome to broaden their use in many applications. Firstly, the large amount of hydroxyl groups on the surface of CNCs make

the nanoparticles present hydrophilic properties, which limits the compatibility between hydrophilic CNCs and a hydrophobic polymeric matrix (Habibi *et al.* 2010; Bagheriasl *et al.* 2015; Morelli *et al.* 2016). In addition, the preparation of CNCs based on sulfuric acid hydrolysis is considered as the most mainstream approach. Negatively charged sulfate esters are introduced on the surface of the obtained CNCs particles when using the sulfuric acid as a hydrolyzing agent. The charged sulfate esters can promote dispersion of the CNCs in water because like charges repel each other. However, the introduction of charged sulfate esters diminishes the thermostability of the nanoparticles, which is attributed to the catalytic nature of sulfate esters (Roman and Winter 2004; Abraham *et al.* 2016). Therefore, two challenges should be overcome in the preparation of nanocomposites reinforced by CNCs, the inferior thermal stability and the obvious hydrophilicity.

There are a large number of reactive hydroxyl groups on the CNCs' surface that can react with different active groups, such as carboxyl, epoxy group, siloxane, *etc.* To improve thermal stability and hydrophobicity, different chemical modification strategies have been attempted, such as esterification (Braun and Dorgan 2009; Sobkowicz *et al.* 2009), oxidation (Shimizu *et al.* 2013, 2014a,b), polymer grafting (Ljungberg *et al.* 2005; Roy *et al.* 2005; Morandiet *et al.* 2009; Goffin *et al.* 2012), *etc.* The resulting nanocrystals show good dispersion abilities in an organic solvent and excellent thermal stability. The goal of these methods was to introduce hydrophobic groups onto the CNCs' surface to replace the hydrophilic hydroxyl groups.

Triazine is an important intermediate in the dye and the pharmaceutical industry. There are three reactive chlorine groups in the chemical structure of 2,4,6-trichloro-1,3,5-triazine (TCT). In this study, triazine derivative was synthesized through the reaction between TCT and BA, and then the derivative was introduced on the CNCs' surface. As shown in Schematic 1, one of the chlorine groups reacted with the hydroxyl groups on the surface of CNCs, and the second chlorine groups reacted with amino groups of aliphatic amine. The hydrophilicity of the nanoparticles diminished and the thermal stability of CNCs was improved due to the hydrophobic aliphatic chains covering the CNCs' surface.



Schematic 1. Synthesis of TCT-BA and its grafting on the surface of CNCs

EXPERIMENTAL

Materials

Cotton, hydrochloric acid, sulfuric acid, acetone, toluene, tetrahydrofuran (THF), sodium hydroxide (NaOH), and sodium bicarbonate were purchased from Sinopharm Chemical Reagent Co., Ltd. (Shanghai, China); TCT was obtained from TCI Shanghai (Shanghai, China) and used to modify the CNCs to improve the reactivity. BA was supplied by J&K Scientific Limited Company (Shanghai, China).

Preparation of cellulose nanocrystals

According to the authors' previous article (Yin *et al.* 2016), CNCs were fabricated from cotton using sulfuric acid hydrolysis. In brief, approximately 10 g of cotton was mixed with 200 mL of sulfuric acid aqueous solution (64 wt.%) in a three-neck flask, which was set with a stirrer, thermometer, and condenser. The reactive mixture was stirred for 1 h at 45 °C for hydrolysis, then approximately 200 mL of cold water (approximately 0 °C) was poured into the obtained suspension to stop the reaction. Subsequently, the suspension was centrifuged at 10,000 rpm until it had no obvious stratification and existed as a kind of transparent dispersion. To remove the sulfate groups on the CNCs' surface, the mixture was neutralized using sodium hydroxide aqueous solution (1 wt.%).

Synthesis of triazine derivative

The triazine derivative was synthesized as follows: first, 7.38 g of TCT and a balanced amount of acetone were added into a 250-mL three-neck round-bottom flask and homogenized with a magnetic stirrer until the triazine was dissolved in the acetone. Next, 3.51 g of BA was added into the above solution dropwise and the reaction was performed at approximately 0 °C to 5 °C for 8 h. The pH of the solution was adjusted to approximately 10 using 10 wt.% NaOH solution. Finally, the triazine derivative, which is named TCT-BA, was obtained after the solution was filtered, washed with 0.1 mol/L hydrochloric acid, 0.1 mol/L sodium bicarbonate, and distilled water, and recrystallized using toluene (Pearlman and Banks 1948).

Modification of cellulose nanocrystals with triazine derivative

The grafting reaction of triazine derivative (TCT-BA) onto CNCs was performed as follows: Briefly, 0.5 g of CNCs was swollen in NaOH solution in the 100-mL three-neck round-bottom flask and stirred at a pH of 10 for 30 min. Then, 0.615 g TCT-BA dissolved in THF was added into the flask dropwise, and the reaction was performed at 40 °C for 4 h. The triazine derivative grafted CNCs (CNC-TCT-BA) were obtained after the solution was filtered, washed with THF and distilled water, and freeze-dried.

Methods

Characterization

Transmission electron microscopy (TEM) was performed using a JEM-2100 electron microscope (Jeol Ltd. USA) operating at an acceleration voltage of 80kV to characterize the morphology and distribution of CNCs.

The chemical structures of the TCT-DA and CNCs before and after modification were characterized on a Bruker 400M solid-state ¹³C NMR spectrometer and a Fourier transform infrared (FT-IR) spectrometer. Infrared spectra were recorded at room temperature on a Nicolet iS 10 Fourier transform infrared spectroscope (FT-IR) (Thermo Fisher Scientific Company, Shanghai, China). The samples were prepared *via* KBr pellet method. The resolution of the spectrometer was 4 cm⁻¹, the wave number range was 400 cm⁻¹ to 4000 cm⁻¹, and the samples were scanned 30 times.

X-ray diffraction (XRD) patterns of CNCs before and after modification were recorded on Bruker Siemens D8 X-ray diffractometer operated at 3 kW with Cu K α radiation ($\lambda=0.154\text{nm}$) in the range $2\theta = 3\sim 60^\circ$ with a step of 0.02° and scanning speed at $4^\circ/\text{min}$.

The grafting efficiency (GE%) of TCT-BA grafted on the surface of CNCs was determined using the Quanta 200 (FEI) electron microscope equipped with the energy

dispersive X-ray (EDX) system. The carbon, oxygen, sulfur, nitrogen, and chlorine elements content for CNC-TCT-BA were measured. TCT-BA-grafting efficiency (GE %) was calculated according to Eq. 1,

$$GE\% \cdot C_{TCT-BA} + (1 - GE\%) \cdot C_{CNC} = C_{CNC-TCT-BA} \quad (1)$$

where C is the relative nitrogen content of the sample.

The thermal degradation of CNCs was analyzed using a thermal analyzer TGA/SDTA851e (Mettler Toledo, Shanghai, China) under nitrogen flow. Approximately 5 mg of dried samples were heated from 30 °C to 600 °C at a heating rate of 10 °C/min.

The contact angle measurement was performed to investigate the hydrophilicity of CNCs before and after modification, which was performed at room temperature using a DSA25S-Kruss contact angle measuring device (Kruss, Beijing, China). The CNCs before and after modification were compacted under 20 MPa to obtain the samples with smooth surfaces. A small drop of water (2 μ L) was dropped on the surface of the samples. Then, the contact angle was calculated using a sessile drop contact angle system.

RESULTS AND DISCUSSION

As shown in Fig. 1, TEM was performed to observe the morphology and dimensions of CNCs. Rod-like nanoparticles were separated from cotton using sulfuric acid hydrolysis. The size of the nanoparticles were 200 nm to 300 nm in length and approximately 10 nm in width, which corresponded to previous literature (Lin *et al.* 2012). According to the TEM images, an agglomeration of nanoparticles was obvious due to the hydrogen bonding between the hydroxyl groups on the CNCs' surface.

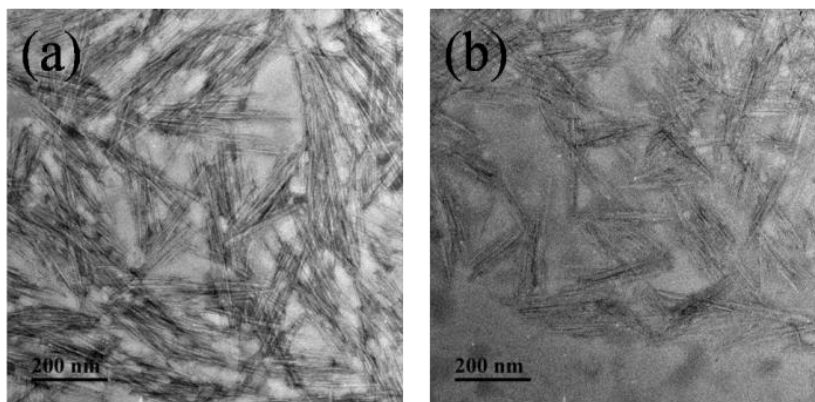


Fig. 1. TEM images of (a) CNCs and (b) CNC-TCT-BA

Fourier transform infrared spectroscopy was performed to analyze the synthesis of triazine derivative and the chemical grafting of CNCs. As shown in Fig. 2, compared with TCT, the spectrum of triazine derivative displayed the characteristic absorption bands of the -NH stretching at 3260 cm^{-1} , bands C=N at 1553 cm^{-1} and 1402 cm^{-1} , and C-Cl stretching at 793 cm^{-1} , which corresponded to the absorption peaks of triazine. The presence of BA was evidenced by the -CH₂ and -CH₃ framework stretching at 2977 cm^{-1} and 2784 cm^{-1} .

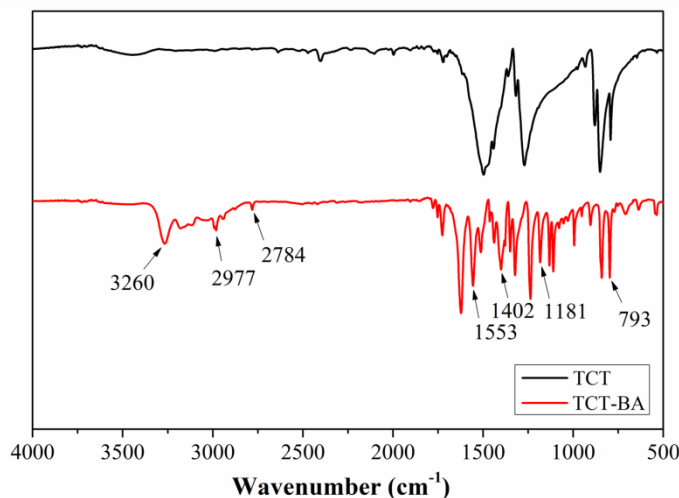


Fig. 2. FTIR spectra of TCT and TCT-BA

To further analyze the chemical structure of TCT and its derivative, ^{13}C NMR was recorded, as shown in Fig. 3. This indicated the successful synthesis of triazine derivative. The TCT-BA displayed typical resonances of TCT and BA. The signals at 172.33 ppm, 164.16 ppm, 158.75 ppm, and 154.59 ppm corresponded to triazine. The signals at $\delta = 15.72$ ppm, 22.04 ppm, 31.00 ppm, and 44.64 ppm were assigned to the carbons on the BA chains at C1, C2, C3, and C4, respectively. The results of the FT-IR and ^{13}C NMR spectra revealed the successful synthesis of triazine derivative.

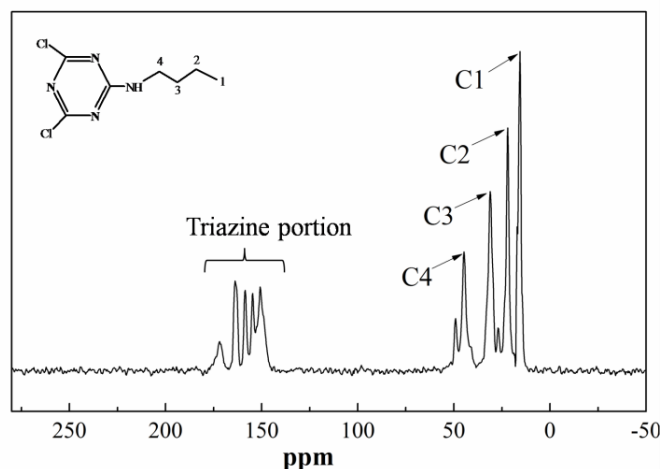


Fig. 3. ^{13}C NMR spectra of TCT-BA

Figure 4 presents the FTIR spectra of CNCs and TCT-BA-grafted CNCs. The spectrum of TCT-BA-grafted CNCs not only showed all of the characteristic absorption peaks of CNCs, but also presented the absorption bands of TCT-BA, such as $-\text{CH}_2$ stretching located at 2854 cm^{-1} , $\text{C}=\text{N}$ stretching at 1583 cm^{-1} , and $\text{C}-\text{Cl}$ stretching situated at 794 cm^{-1} . The successful grafting of TCT-BA on the CNCs surface was further confirmed using ^{13}C NMR, as shown in Fig. 5. The signals at $\delta = 105.01$ ppm, 71.50 ppm, 72.98 ppm, 89.25 ppm, 75.44 ppm, and 65.36 ppm were assigned to the carbons on the glucose ring at C1, C2, C3, C4, C5, and C6, respectively. The signals at 152.33 ppm and

150.39 ppm corresponded to signals of triazine. The ^{13}C NMR spectrum of CNC-TCT-BA also showed signals at $\delta = 14.30$ ppm, 29.10 ppm, and 45.15 ppm corresponding to the carbons on the BA chains at C7, C8, C9, C10, respectively. The results of FTIR and ^{13}C NMR confirmed the successful grafting of TCT-BA onto CNCs.

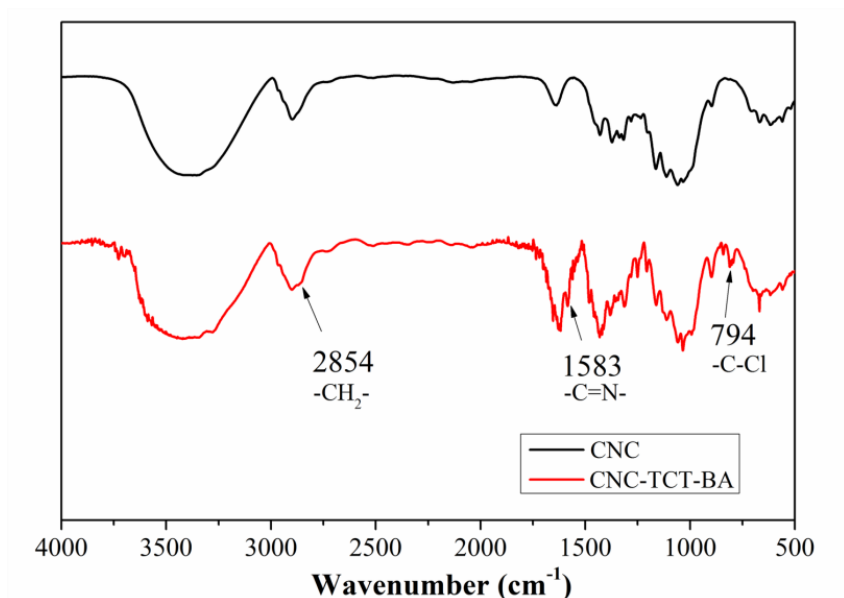


Fig. 4. FTIR spectra of CNCs and CNC-TCT-BA

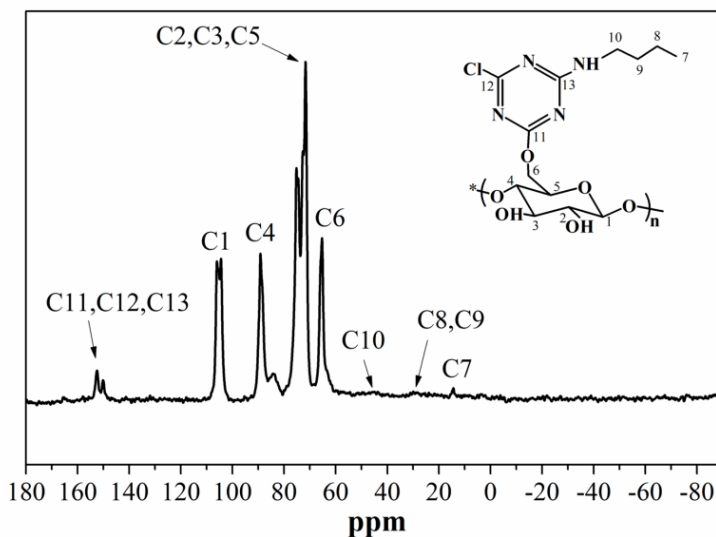


Fig. 5. ^{13}C NMR spectrum of the CNC-TCT-BA

The EDX spectrum of unmodified and CNCs modified with TCT-BA (Fig. 6) indicated that the grafting efficiency (GE%) of TCT-BA on the CNCs surface was 35.9%. It also revealed that the sulfate esters were partly replaced or covered by TCT-BA after modification because sulfur element was decreased in the chemical structure on TCT-BA-modified CNCs. Therefore, the thermal stability of TCT-BA-grafted CNCs was improved significantly, which was attributed to the replacement and/or cover of sulfate esters on the surface of nanoparticles.

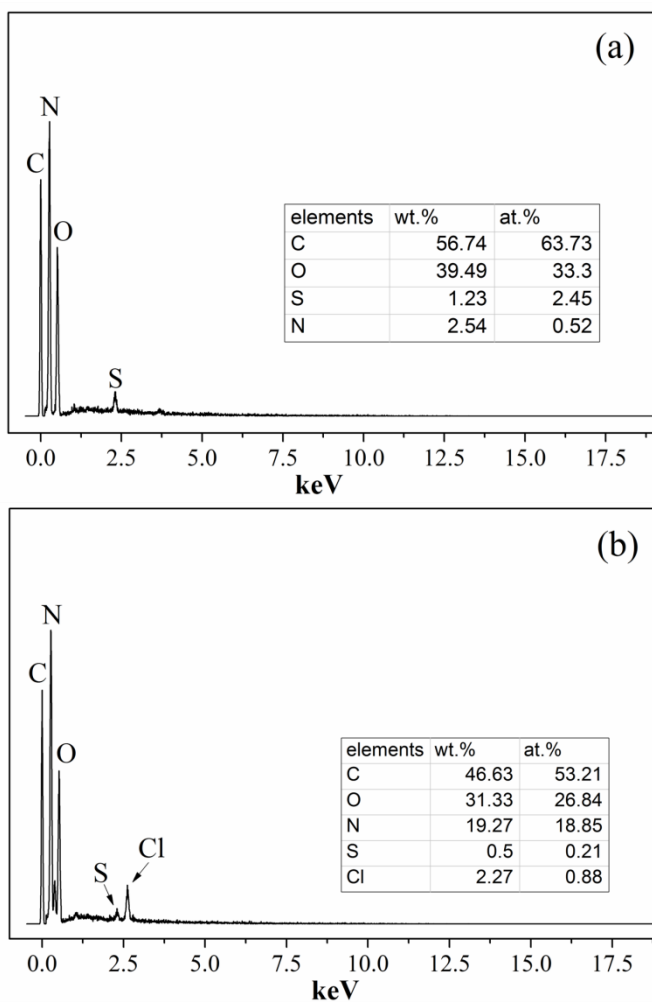


Fig. 6. EDX spectrum of (a) CNCs; and (b) CNC-TCT-BA

X-ray diffraction patterns of unmodified CNCs and modified CNCs are presented in Fig. 7.

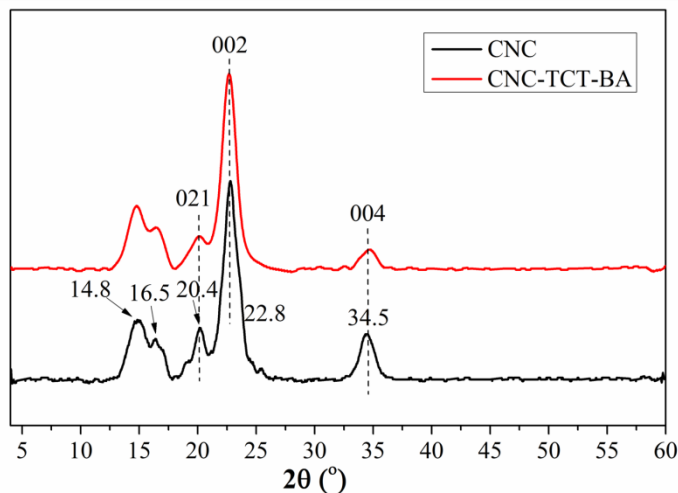


Fig. 7. XRD spectra of CNCs before and after modification

Both of the samples represented the peaks at $2\theta=14.8^\circ$ (101), $2\theta=16.5^\circ$ ($10\bar{1}$), $2\theta=22.8^\circ$ (002), and $2\theta=34.5^\circ$ (040), which corresponded to the crystalline structure of cellulose I of the polymorphous of cellulose (Wong *et al.* 2009). Comparing with the pristine nanocrystals, the diffraction intensity of the modified CNCs was obviously reduced and the half-peak width became broader. The peaks of CNC-TCT-BA assigned to (021), (002), and (004) planes became weaker than CNCs, indicating that modification occurred not only in amorphous regions but also in the edge of crystalline regions.

To analyze the compatibility of CNCs, water contact angle measurements were performed as shown in Fig. 8. It was obvious that unmodified CNCs, with an initial contact angle of 50° , presented good hydrophilicity.

Compared with unmodified CNCs, the contact angle of modified CNCs was increased approximately 40° . This result revealed that the nanoparticles modified with TCT-BA became more hydrophobic than pure CNCs, which was attributed to the hydrophobic BA chains on the CNCs' surface.

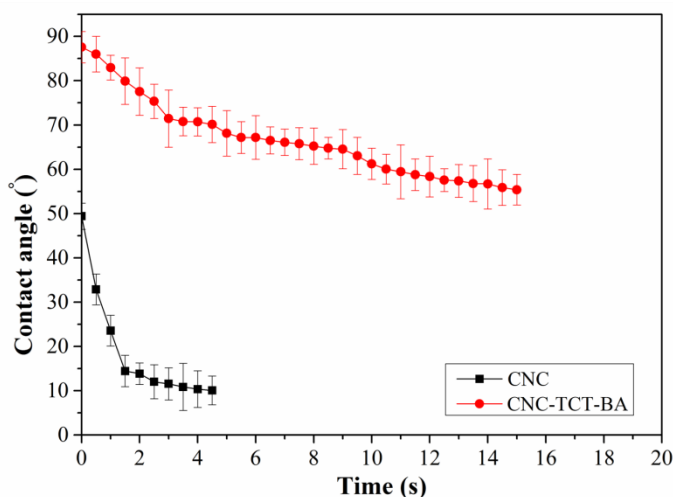


Fig. 8. Dynamic contact angle curves of CNCs and CNCs modified with TCT-BA

Figure 9 presents the thermal stability of CNCs before and after modification. The CNCs clearly presented a stepwise degradation behavior, and it involved three processes. The degradation processes, which started below 150°C for both of the samples, were attributed to the evaporation of adsorbed water. The degradation of pure CNCs between 200°C and 400°C presented two processes. The lower temperature degradation process corresponded to degradation of the amorphous regions, where the material was more accessible and more highly sulfated, whereas the higher temperature degradation process related to the breakdown of the nonsulfated crystalline interior (Roman and Winter 2004; Martinez-Sanz *et al.* 2011).

Compared with unmodified CNCs, the initial decomposition of TCT-BA-grafted CNCs shifted from 190°C to 340°C , which indicated that the thermal stability of CNCs modified with TCT-BA was remarkably improved. This was attributed to the shielding effect of the sulfate groups and the increase of crystallinity, which was corresponded with the previous report (Maiti *et al.* 2013).

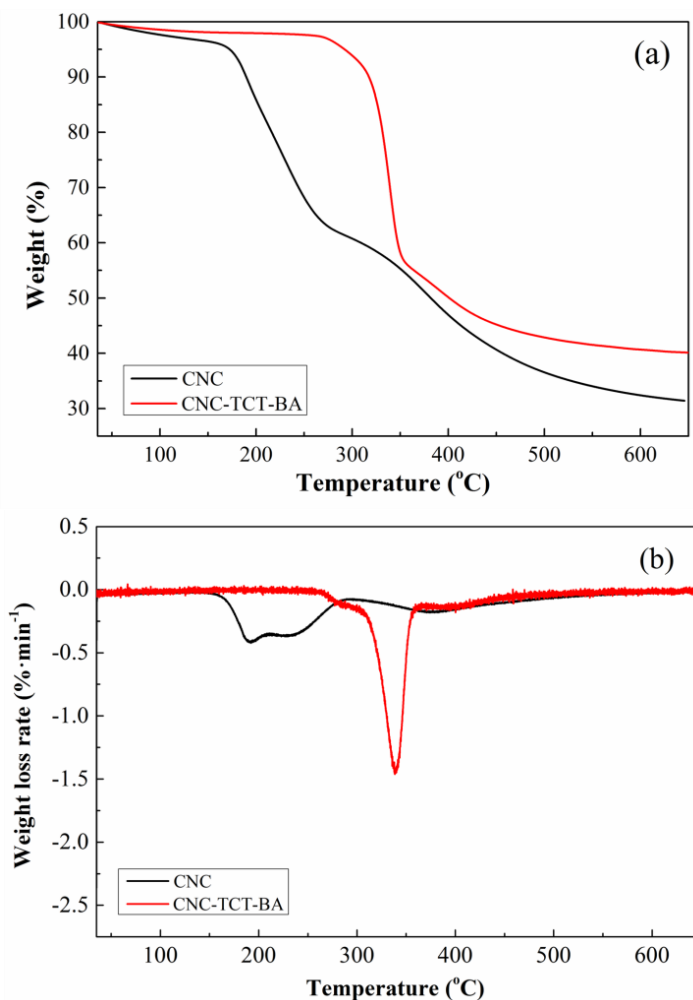


Fig. 9. Curves of: (a) TGA of CNCs and CNC-TCT-BA; and (b) DTG of CNCs and CNC-TCT-BA

CONCLUSIONS

1. Triazine derivative was successfully synthesized and innovatively grafted onto the surface of CNCs.
2. Compared with pure CNCs, the onset decomposition temperature of modified CNCs was increased by 150 °C. The hydrophilicity of the modified nanoparticles decreased, which was attributed to the hydrophobic triazine derivative that covered CNCs' surface.
3. This study provided a new solution to the modification of CNCs that is economical and effective.

ACKNOWLEDGEMENTS

The authors are grateful to the National Natural Science Foundation of China (Grant Nos. 31570578 and 31270632), the Fundamental Research Funds for the Central Universities (Grant No. JUSRP51622A), the Graduate Student Innovation Plan of the

Jiangsu Province of China (KYLX16_0790), and the fund supported by the China Scholarship Council.

REFERENCES CITED

- Abraham, E., Kam, D., Nevo, Y., Slattegard, R., Rivkin, A., Lapidot, S., and Shoseyov, O. (2016). "Highly modified cellulose nanocrystals and formation of epoxy-nanocrystalline cellulose (CNC) nanocomposites," *ACS Appl. Mater. Inter.* 8(41), 28086-28095. DOI: 10.1021/acsami.6b0985
- Annadurai, G., Juang, R. S., and Lee, D. J. (2002). "Use of cellulose-based wastes for adsorption of dyes from aqueous," *J. Hazard. Mater.* 92(3), 263-274. DOI:10.1016/S0304-3894(02)00017-1
- Azouz, K. B., Ramires, E. C., Fonteyne, W. V., Kissi, N. E., and Dufresne, A. (2012). "Simple method for the melt extrusion of a cellulose nanocrystal reinforced hydrophobic polymer," *ACS Macro. Lett.* 1(1), 236-240. DOI: 10.1021/mz2001737
- Bagheriasl, D., Carreau, P. J., Dubois, C., and Riedl, B. (2015). "Properties of polypropylene and polypropylene/poly(ethylene-co-vinyl alcohol) blend/CNC nanocomposites," *Compos. Sci. Technol.* 117, 357-363. DOI: 10.1016/j.compscitech.2015.07.012
- Bake, C., Hanif, Z., Cho, S. W., Kim, D. I., and Um, S. H. (2013). "Shape control of cellulose nanocrystals via compositional acid hydrolysis," *J. Biomed. Nanotechnol.* 9(7), 1293-1298. DOI: 10.1166/jbn.2013.1535
- Braun, B., and Dorgan, J. R. (2009). "Single-step method for the isolation and surface functionalization of cellulosic nanowhiskers," *Biomacromolecules* 10(2), 334-341. DOI: 10.1021/bm8011117
- Chen, L., Wang, Q., Hirth, K., Baez, C., Agarwal, U. P., and Zhu, J. Y. (2015). "Tailoring the yield and characteristics of wood cellulose nanocrystals (CNC) using concentrated acid hydrolysis," *Cellulose* 22(3), 1753-1762. DOI: 10.1007/s10570-015-0615-1
- Goffin, A. L., Habibi, Y., Raquez, J. M., and Dubois, P. (2012). "Polyester-grafted cellulose nanowhiskers: A new approach for tuning the microstructure of immiscible polyester blends," *ACS Appl. Mater. Inter.* 4(7), 3364-3371. DOI: 10.1021/am3008196
- Guo, J., Guo, X., Wang, S., and Yin, Y. (2016). "Effects of ultrasonic treatment during acid hydrolysis on the yield, particle size and structure of cellulose nanocrystals," *Carbohydr. Polym.* 135(4), 248-255. DOI: 10.1016/j.carbpol.2015.08.068
- Habibi, Y., Goffin, A. L., Schiltz, N., Duquesne, E., Dubois, P., and Dufresne, A. (2008). "Bionanocomposites based on poly(ϵ -caprolactone)-grafted cellulose nanocrystals by ring-opening polymerization," *J. Mater. Chem.* 18(41), 5002-5010. DOI: 10.1039/B809212E
- Habibi, Y., Lucia, L. A., and Rojas, O. J. (2010). "Cellulose nanocrystals: Chemistry, self-assembly, and applications," *Chem. Rev.* 110(6), 3479-3500. DOI: 10.1021/cr900339w
- Iwamoto, S., Kai, W., and Iwata, T. (2009). "Elastic modulus of single cellulose microfibrils from tunicate measured by atomic force microscope," *Biomacromolecules* 10(9), 2571-2576. DOI: 10.1021/bm900520n

- Jokerst, J. V., Bohndiek, S. E., and Gambhir, S. S. (2014). "Cellulose nanoparticles: Photoacoustic contrast agents that biodegrade to simple sugars," *SpieProceedings* 8943(15), 131-135. DOI: 10.1117/12.2036256
- Klemm, D., Schumann, D., Udhardt, U., and Marsch, S. (2001). "Bacterial synthesized cellulose-artificial blood vessels for microsurgery," *Prog. Polym. Sci.* 26(9), 1561-1603. DOI: 10.1016/S0079-6700(01)00021-1
- Lin, N., and Dufresne, A. (2013). "Physical and/or chemical compatibilization of extruded cellulose nanocrystal reinforced polystyrene nanocomposites," *Macromolecules* 46(14), 5570-5583. DOI: 10.1021/ma4010154
- Lin, N., Huang, J., and Dufresne, A. (2012). "Preparation, properties and application of polysaccharide nanocrystals in advanced functional nanomaterials: A review," *Nanoscale* 4(11), 3274-3294. DOI: 10.1039/c2nr30260h
- Liu, J. H., Yang, R., Wang, F. M., Zhao, Q., and Cheng, H. (2014). "Technology optimization of enzymolysis of Bermuda grass," *Res. J. Appl. Sci. Eng. Technol.* 7(12), 2411-2415. DOI: 10.19026/rjaset.7.544
- Liu, Y., Li, Y., Yang, G., Zheng, X. T., and Zhou, S. B. (2015). "Multi-stimulus-responsive shape-memory polymer nanocomposite network cross-linked by cellulose nanocrystals," *ACS Appl. Mater. Inter.* 7(7), 4118-4126. DOI: 10.1021/am5081056
- Ljungberg, N., Bonini, C., Bortolussi, F., Boisson, C., Heux, L., and Cavaille, J. Y. (2005). "New nanocomposite materials reinforced with cellulose whiskers in atactic polypropylene: Effect of surface and dispersion characteristics," *Biomacromolecules* 6(5), 2732-2739. DOI: 10.1021/bm050222v
- Maiti, S., Jayaramudu, J., Das, K., Reddy, S. M., Sadiku, R., Ray, S. S., and Liu, D. (2013). "Preparation and characterization of nano-cellulose with new shape from different precursor," *Carbohydr. Polym.* 98(1), 562-567. DOI: 10.1016/j.carbpol.2013.06.029
- Martinez-Sanz, M., Lopez-Rubio, A., and Lagaron, J. M. (2011). "Optimization of the nanofabrication by acid hydrolysis of bacterial cellulose nanowhiskers," *Carbohydr. Polym.* 85(1), 228-236. DOI: 10.1016/j.carbpol.2011.02.021
- Morelli, C. L., Belgacem, N., Branciforti, M. C., Salon, M. C. B., Bras, J., and Bretas, R. E. S. (2016). "Nanocomposites of PBAT and cellulose nanocrystals modified by *in situ* polymerization and melt extrusion," *Polym. Eng. Sci.* 56(12), 1339-1348. DOI: 10.1002/pen.24367
- Morandi, G., Heath, L., and Thielemans, W. (2009). "Cellulose nanocrystals grafted with polystyrene chains through surface-initiated atom transfer radical polymerization (SI-ATRP)," *Langmuir* 25(14), 8280-8286. DOI: 10.1021/la900452a
- Pearlman, W. M., and Banks, C. K. (1948). "Substituted chlorodiamino-s-triazines," *J. Am. Chem. Soc.* 70(11), 3726-3728. DOI: 10.1021/ja01191a053
- Roman, M., and Winter, W. T. (2004). "Effect of sulfate group from sulfuric acid hydrolysis on the thermal degradation behavior of bacterial cellulose," *Biomacromolecules* 5(5), 1671-1677. DOI: 10.1021/bm034519+
- Roy, D., Guthrie, J. T., and Perrier, S. (2005). "Graft polymerization: Grafting poly(styrene) from cellulose *via* reversible addition-fragmentation chain transfer (ATRP) polymerization," *Macromolecules* 38(25), 10363-10372. DOI: 10.1021/ma0515026
- Shimizu, M., Fukuzumi, H., Saito, T., and Isogai, A. (2013). "Preparation and characterization of TEMPO-oxidized cellulose nanofibrils with ammonium

- carboxylate groups,” *Int. J. Biol. Macromol.* 59, 99-104. DOI: 10.1016/j.ijbiomac.2013.04.021
- Shimizu, M., Saito, T., Fukuzumi, H., and Isogai, A. (2014a). “Hydrophobic, ductile, and transparent nanocellulose films with quaternary alkylammonium carboxylates on nanofibril surfaces,” *Biomacromolecules* 15(11), 4320-4325. DOI: 10.1021/bm501329v
- Shimizu, M., Saito, T., and Isogai, A. (2014b). “Bulky quaternary alkylammonium counterions enhance the nanodispersibility of 2,2,6,6-tetramethylpiperidine-1-oxyl-oxidized cellulose in diverse solvents,” *Biomacromolecules* 15(5), 1904-1909. DOI: 10.1021/bm500384d
- Sobkowicz, M. J., Braun, B., and Dorgan, J. R. (2009). “Decorating in green: Surface esterification of carbon and cellulosic nanoparticles,” *Green Chem.* 11, 680-682. DOI: 10.1039/B817223D
- Wong, S.S., Kasapis, S., and Tan, Y. M. (2009). “Bacterial and plant cellulose modification using ultrasound irradiation,” *Carbohydr. Polym.* 77(2), 283-287 DOI: 10.1016/j.carbpol.2008.12.038
- Yin, Y. Y., Tian, X. Z., Jiang, X., Wang, H. B., and Gao, W. D. (2016). “Modification of cellulose nanocrystal *via* SI-ATRP of styrene and the mechanism of its reinforcement of polymethylmethacrylate,” *Carbohydr. Polym.* 142, 206-212. DOI: 10.1016/j.carbpol.2016.01.014
- Zhang, C. M., Salick, M. R., Cordie, T. M., Ellingham, T., Dan, Y., and Turng, L. (2015). “Incorporation of poly(ethylene glycol) grafted cellulose nanocrystals in poly(lactic acid) electrospun nanocomposite fibers as potential scaffolds for bone tissue engineering,” *Mat. Sci. Eng. C-Mater. Biol. Appl.* 49, 463-471. DOI: 10.1016/j.msec.2015.01.024

Article submitted: April 11, 2017; Peer review completed: July 22, 2017; Revised version received and accepted: August 15, 2017; Published: August 23, 2017.
DOI: 10.15376/biores.12.4.7427-7438